INHERENT OPTICAL PROPERTIES IN NEW ENGLAND COASTAL WATERS: DECOMPOSITION INTO CONTRIBUTIONS FROM OPTICALLY IMPORTANT CONSTITUENTS

Morrison, J. R. and Sosik, H. M.
Woods Hole Oceanographic Institution, Woods Hole, MA 02543

ABSTRACT

The optical properties of case II coastal ocean waters are influenced by a complex mixture of seawater constituents and by a wide variety of physical processes. Especially in regions where formation of physical and optical fronts is frequent, but temporally and spatially variable, this complexity makes interpretation of ocean color signals subject to large uncertainty. The goal of our research is to determine which processes and optically important constituents must be considered to explain ocean color variations associated with coastal fronts on the New England continental shelf. To accomplish this goal we have implemented extensive time series sampling to support algorithm development and evaluation as a component of the NOPP-supported FRONT program. The FRONT study site is located at the mouth of Long Island Sound, an area strongly affected by estuarine outflow and tidal currents. Here we present inherent optical property (IOP) data collected with a WetLabs ac-9 absorption and attenuation meter from deployments of a custom designed mooring, the Autonomous Vertically Profiling Plankton Observatory (AVPPO). We developed a new method, which is independent of near infrared absorption measurements, to correct ac-9 absorption measurements for the effects of scattering. This new method has advantages because previous scattering correction approaches were limited by variability at near infrared wavelengths that cannot be explained by temperature and salinity corrections. Scattering corrected absorption spectra were decomposed into algal and non-algal fractions based on characteristic shapes of spectral absorption for the constituents. The strong relationship between scattering and the non-algal absorption allowed the separation of absorption from Colored Dissolved Organic Matter (CDOM) and from non-algal particles. We present distributions of absorption by these bio-optically important constituents (phytoplankton, non-algal particles, and CDOM). Optical constituents varied with tidal, seasonal, and external forcing. Diurnal variation was also evident in phytoplankton optical properties in surface waters.

INTRODUCTION

The color of the ocean, as detected from above, depends strongly on the Inherent Optical Properties (IOPs) of the of the upper water column. IOPs include the absorption and scattering coefficients, *a* and *b*, respectively. The magnitude and spectral dependence of these coefficients are determined not only by seawater, but also by optically important constituents, which include phytoplankton, colored dissolved organic matter (CDOM), and non-algal particles. Seawater, phytoplankton and non-algal particulates both absorb and scatter light whereas CDOM is an important absorber but contributes negligibly to scattering (Mobley 1994).

The WetLabs ac-9 meter measures the absorption and attenuation coefficients (due to constituents other than water) at 9 wavelengths in the visible and near infrared (412, 449, 488, 510, 532, 555, 630, 676, and 715 nm). Obtaining accurate results from ac-9 data requires three important processing steps; 1) correcting the absorption for temperature and salinity effects (Pegau et al. 1997), 2) correcting absorption measurements for scattering artifacts (Zaneveld et al. 1994), and 3) correction of both absorption and scattering for instrument drifts since the last manufacturer's calibration determined using pure water calibrations (Twardowski et al. 1999). All methods for the scattering correction of the absorption measurements assume that the absorption at 715 nm can be adequately corrected for temperature and salinity effects and that true absorption at 715 nm is negligible. Any signal at this wavelength remaining after temperature and salinity correction is thus assumed to be due to scattering. In the simplest scattering correction approach, this signal is used as a wavelength independent offset. The temperature correction factor is the product of the temperature correction coefficient, Ψ_T, and the difference between manufacturer calibration and water temperatures. Unfortunately, the large magnitude and strong wavelength dependence of Ψ_T at near 715 can cause potential errors. A ± 2 nm uncertainty in the central wavelength of an interference filter at 715 nm can give greater than a 50 % error in Ψ_T (Pegau et al. 1997). This equates to a difference of 0.01 m^{-1} for a 10 ºC difference between calibration and sample water temperatures which can be significant, especially in clear waters. The scattering correction is also complicated by the non-negligible absorption at 715, especially by particles. Analysis of 854 Quantitative Filter technique (QFT) particulate absorption spectra, $a_p(\lambda)$, from the North East Atlantic, obtained from the NASA SeaBASS database, showed that 838 had $a_p(715)$ greater than zero. On average $a_p(715)$ was 12.5 (σ=5) % of the magnitude of $a_p(550)$.

Fronts in the coastal ocean are areas of strong horizontal, and potentially vertical, gradients in both biological and physical properties (Simpson and Bowers 1981; O'Donnell 1993). As such, they can provide a wide range in optically important constituents and IOPs. The National Ocean Partnership Program (NOPP) Front Resolving Observational Network With Telemetry (FRONT) site is located at the mouth of Long Island sound; this site was selected for further study after the analysis of 12 years of AVHRR data showed the region to be an area of strong frontal activity (Ullman and Cornillon 1999). The Autonomous Vertically Profiling Plankton Observatory (AVPPO) (Thwaites et al. 1998) was deployed twice at the FRONT site (FRONT1 and FRONT4) and in Massachusetts Bay during 2000 and 2001 (Table 1). The AVPPO consists of buoyant sampling vehicle and a trawl-resistant bottom-mounted enclosure, which holds a winch, the vehicle (when not sampling), batteries, and controller. Three sampling systems are present on the vehicle, a video plankton recorder, a CTD with accessory sensors, and a suite of bio-optical sensors including Satlantic OCI-200 and OCR-200 spectral radiometers and a WetLabs ac-9 absorption and attenuation meter. Data from the bio-optical sensors is collected on a custom built data acquisition module that incorporates a time stamp into all data streams. At preprogrammed times the vehicle is released, floats to the surface, and is then winched back into the enclosure with power and data connection maintained through the winch cable. Communication to shore is possible through a nearby surface telemetry buoy, equipped with a mobile modem; this

provides the capability for near-real time data transmission and interactive sampling control.

Table 1: AVPPO deployment locations and dates.

Name	Location	Latitude	Longitude	Dates of data
FRONT1	Mouth of Long Island Sound	40.9922 °N	79.7332 ° W	9-12 December 2000
MassBay	Massachusetts Bay	42.2423 °N	70.5571 °W	13-17 September 2001
FRONT4	Mouth of Long Island Sound	40.9864 °N	71.7472 °W	13-24 November 2001

SCATTERING CORRECTION AND ABSORPTION DECOMPOSITION

Data from the ac-9 mounted on the AVPPO was initially merged with that from environmental sensors based on time. A time offset was determined by comparing depth measurements from the two data sets. The absorption and attenuation measurements were corrected for temperature and salinity variations as detailed in Pegau et al. (1997). For each profile the data was averaged into one-meter bins.

A simple model of the absorption measured by an ac-9, $a_{ac9}(\lambda)$, is the sum of absorption by phytoplankton and non-algal matter plus a scattering offset, $a_b(\lambda)$. In addition the absorption by phytoplankton, $a_{ph}(\lambda)$, can be approximated as the product of a chlorophyll specific absorption coefficient, $a_{ph}^*(\lambda)$, and the chlorophyll concentration, *Chl*. Both non-algal particles and CDOM show a characteristic exponential decrease in absorption with increasing wavelength (e.g. Roesler et al. 1989). The combined absorption by non-algal particles and CDOM, $a_{dm}(\lambda)$, can be modeled in terms of an absorption at a reference wavelength, $a_{dm}(\lambda_0)$, and a slope term, *S*. Thus

$$a_{ac9}(\lambda) = Chl.a^*_{ph}(\lambda) + a_{dm}(\lambda_0)\,exp[-S(\lambda - \lambda_0)] + a_b(\lambda) \quad (1)$$

If $a_b(\lambda)$ is assumed to be wavelength independent, then, given $a_{ac9}(\lambda)$, $a_{ph}^*(\lambda)$ and *S*, it is possible to estimate *Chl*, $a_{dm}(\lambda_0)$, and a_b with multiple linear regression.

Equation 1 was used as the basis for an iterative new scattering correction approach. The iteration involved looping over two main steps until a termination criterion was met. At the start of the correction process initial values are required for $a_{ph}^*(\lambda)$, and *S*; these can be determined from average properties of discrete water samples analyzed from the study site. Using the all ac-9 wavelengths except 715 nm, initial values of *Chl*, $a_{dm}(\lambda_0)$, and a_b were calculated using multiple linear regression. These initial estimates of *Chl* and $a_{dm}(\lambda_0)$ were discarded, and $a_{ac9}(\lambda)$ was initially corrected by subtracting a_b from all wavelengths. In the absence of the scattering term Equation 1 simplifies to that describing the desired ac-9 measurement, the total absorption in the absence of water, $a_{nw}(\lambda)$.

$$a_{nw}(\lambda) = a_{ac9}(\lambda) - a_b(\lambda) = C.a^*_{ph}(\lambda) + a_{dm}(\lambda_0)\,exp[-S(\lambda - \lambda_0)] \quad (2)$$

A spectral decomposition was then used to obtain estimates for *Chl*, $a_{dm}(\lambda_0)$, and *S* by minimization of the sum of square deviation between the initial estimate of $a_{nw}(\lambda)$ and a value predicted by iteratively varying *Chl*, $a_{dm}(\lambda_0)$, and *S*. A predicted $a_{dm}(\lambda)$ was calculated using the retrieved values of $a_{dm}(\lambda_0)$, and *S*, and a predicted $a_{ph}(\lambda)$ was calculated as the difference between $a_{nw}(\lambda)$ and $a_{dm}(\lambda)$.

Thus at the end of the first loop, new spectral shapes were derived for the non-algal and phytoplankton absorption, described by *S* and $a_{ph}(\lambda)$, respectively. A new $a_{ph}^*(\lambda)$ was obtained by scaling $a_{ph}(\lambda)$ such that $a_{ph}^*(675)$ was 0.02 mgm^{-2}. These new values were then used as the initial estimates for the start of a new loop. This was repeated *i* times until

$$\sum_{\lambda=1}^{8}(a_{ph}^*(\lambda)_i - a_{ph}^*(\lambda)_{i-1})^2 \Big/ \sum_{\lambda=1}^{8} a_{ph}^*(\lambda)_{i-1} < tol \qquad (3)$$

where *tol* represents a tolerance, which was set in this study at 0.01. The emphasis in this study was placed on retrieving $a_{ph}(\lambda)$. In waters where non-algal absorption dominates, the a_{ph} terms in Equation 3 could be replaced by a_{dm} or a combination of parameters could be used. The $a_{ph}^*(\lambda)$ could also be fixed to prevent major deviation of $a_{ph}(\lambda)$ from the average shape (some deviation is still possible due to the way $a_{ph}(\lambda)$ is calculated).

The resulting a_{nw}, a_{dm}, and a_{ph}, spectra were compared with those obtained using a Lambda-18 spectrophotometer (Perkin-Elmer) and discrete water samples. $a_p(\lambda)$ was measured using the Quantitative Filter Technique (QFT) (Mitchell 1990) and $a_d(\lambda)$ was measured after methanol extraction of the phytoplankton pigments. $a_{ph}(\lambda)$ was calculated as the difference between $a_p(\lambda)$ and $a_d(\lambda)$. $a_{CDOM}(\lambda)$ was measured referenced to optically clean water using matched 10 cm quartz windowed cells. Particulate and dissolved spectra were offset to zero using the mean absorption over a 10 nm window centered at 750 and 670 nm respectively. The discrete water sample spectra were also compared with a_{nw}, a_{dm}, and a_{ph} spectra calculated using the Zaneveld et al. (1994) proportional method scattering correction and subsequent spectral decomposition summarized in Equation 2 and the paragraph thereafter. Initial results indicated that the Zaneveld et al. proportional methods correction introduced a significant offset, of the order of 10 % of the maximum absorption, in both $a_{nw}(\lambda)$ and $a_{ph}(\lambda)$ which were not present using the new correction (Table 2).

Table 2: Results of regression analyses comparing absorptions measured using a spectrophotometer and the ac-9 corrected for scattering using the Zaneveld et al. (1994) proportion method and the new correction. Both a_{nw} and a_{ph} had significant offsets with the proportion method which were 7 and 14 % of the maximum values, respectivley. The slope t and p values are for a comparison to a slope of 1.

		Intercept	*t*	*p*	slope	*t*	*p*	r^2
Zaneveld proportion method	a_{nw}	0.032 (0.004)	8.68	0.000	1.049 (0.021)	2.33	0.023	0.976
	a_{dm}	0.011 (0.004)	2.96	0.004	0.998 (0.027)	0.07	0.941	0.955
	a_{ph}	0.020 (0.003)	7.54	0.000	1.183 (0.060)	3.05	0.003	0.862
New correction	a_{nw}	0.008 (0.004)	1.93	0.058	1.098 (0.025)	3.92	0.000	0.968
	a_{dm}	0.011 (0.004)	2.86	0.006	1.161 (0.030)	5.37	0.000	0.961
	a_{ph}	0.001 (0.001)	0.82	0.415	0.837 (0.029)	5.62	0.000	0.933

Because the ac-9 derived total scattering coefficient (without water, $b_{nw}(\lambda)$) was correlated with the non-aglal absorption (Figure 1), we were able to estimate scattering by different constituents. The scattering coefficient of a constituent, like the absorption coefficient, can be represented by the product of a concentration specific coefficient and the concentration. Alternatively, the absorption of a constituent at a discrete wavelength may be considered as a proxy for concentration. The non-water scattering, $b_{nw}(\lambda)$ (the sum of scattering due to phytoplankton, $b_{ph}(\lambda)$, and non-algal scattering, $b_d(\lambda)$) can then be expressed in terms of spectral absorption specific scattering coefficients for both phytoplankton, $b_{ph}^{*,aph}(\lambda)$, and non-algal matter, $b_d^{*,ad}(\lambda)$:

$$b_{nw}(\lambda) = b_{ph}(\lambda) + b_d(\lambda) = a_{ph}(440).b_{ph}^{*,aph}(\lambda) + a_d(440).b_d^{*,ad}(\lambda). \quad (4)$$

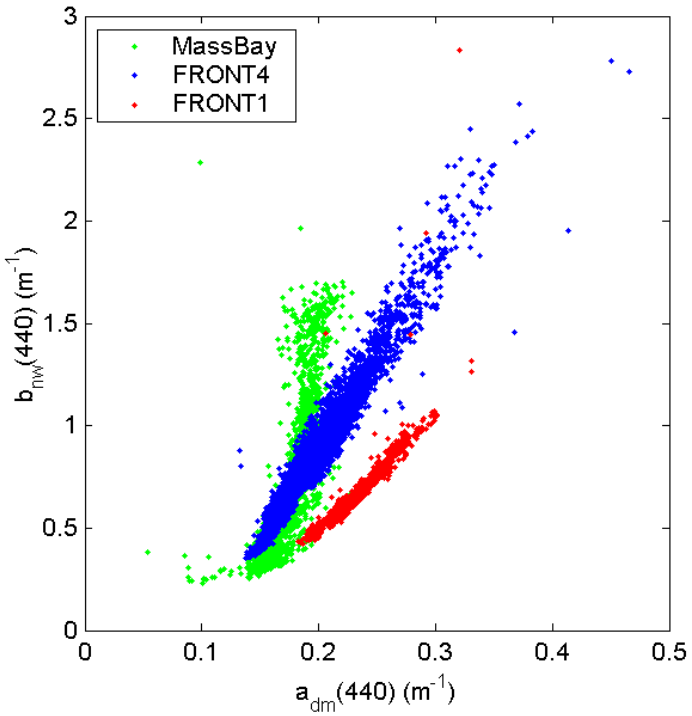

Figure 1: Non-water scattering, b_{nw}, was correlated to the non-algal absorption at 440 nm.

To estimate the scattering due to phytoplankton, a_{dm} was substituted for a_d in Equation 4. The specific scattering coefficients, calculated for each deployment using multiple linear regression, showed typical spectral shapes for both non-algal particle and phytoplankton scattering (Figure 2). For all wavelengths and all deployments greater than 80% of the variability of b_{nw} was explained by the regression. Assuming that CDOM does not scatter, $b_d(\lambda)$ was then calculated by subtracting $b_{ph}(\lambda)$, estimated using $a_{ph}(440)$ and the regression $b_{ph}^{*,aph}(\lambda)$, from the total scattering. A further simplification is to assume that CDOM does not covary with non-algal particles and that variability in $a_{dm}(\lambda)$ is dominated by $a_d(\lambda)$. In this case $a_{dm}(\lambda)$ can be approximated in terms of b_d at a

reference wavelength, the spectral scattering specific absorption coefficients, $a_d^{*,b}(\lambda)$, and the mean CDOM absorption, $\bar{a}_{CDOM}(\lambda)$, for a given data set:

$$a_{dm}(\lambda) = b_d(410)a_d^{*,b}(\lambda) + \bar{a}_{CDOM}(\lambda) \quad (5)$$

$a_{dm}(\lambda)$ was calculated using $a_d^{*,b}(\lambda)$,estimated for each deployment by linear regression, and $b_d(410)$. Finally, $a_{CDOM}(\lambda)$ was calculated as the difference between $a_{dm}(\lambda)$ and $a_d(\lambda)$. This effectively assigns the intercept and the residuals from the regressions to $a_{CDOM}(\lambda)$.

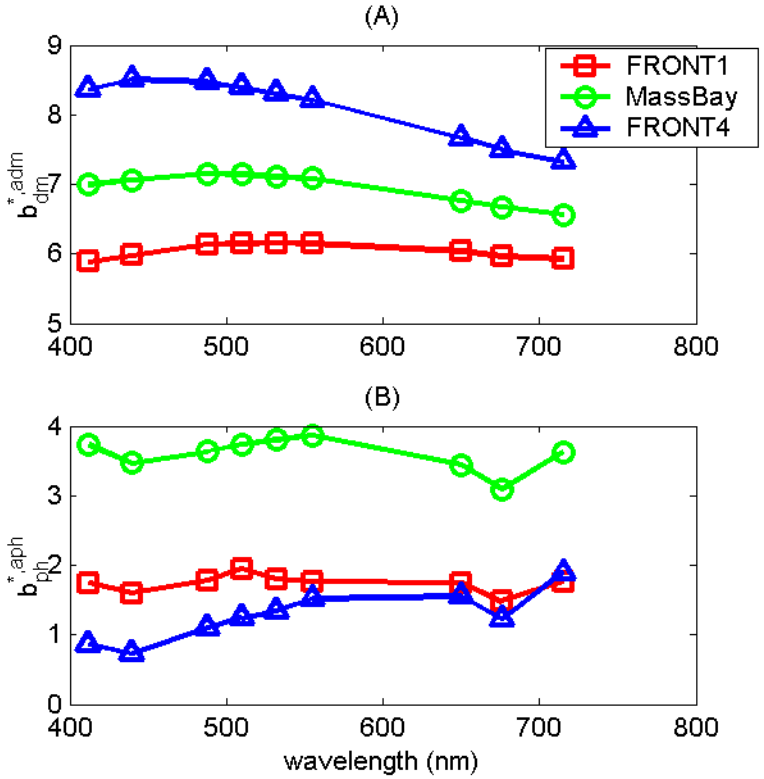

Figure2: Spectral absorption specific scattering coefficients for, A) non-algal matter, $b_d^{*,adm}(\lambda)$, and B) phytoplankton, $b_{ph}^{*,aph}(\lambda)$. The decreased scattering associated with phytoplankton absorption peaks can clearly be seen in $b_{ph}^{*,aph}(\lambda)$. At all wavelengths the multiple regression used to calculate the specific scattering coefficients explained greater than 80% of the non-water scattering variability.

CONSTITUENT DISTRIBUTIONS

The constituent concentration distributions differed for each of the deployments (Figure 3). Seasonal variations were evident in the distributions from the two FRONT deployments. Phytoplankton absorption was greater during FRONT4 than FRONT1, which may be indicative of a higher biomass during the fall deployment. The a_d distribution was approximately the same for both deployments. Resuspension may be the dominant source of non-algal particles at the FRONT site and this result suggests that the amount of resuspension was similar in both seasons. CDOM concentrations were higher during the winter FRONT1 deployment. Expected similarities exist between all three deployments; a_{ph} values were greater in surface waters (Figure 4A-C) and, all a_d

distributions showed increases towards the bottom probably associated with resuspension of sediments (Figure 4 D-F). During the MassBay deployment, the deepening of the surface mixed layer associated with the propagation of internal waves was evident in all three IOPs. Variations in the IOPs on tidal timescales were evident during FRONT1, most clearly in a_d and a_{CDOM}. a_{ph} appeared to reach a maximum at noon each day; this apparent diel variation was not evident in the absorption by other constituents. Analysis of the mean $a_{ph}(\lambda)$ in the top 20 m from the FRONT4 deployment showed variation on diel time scales, not only in the magnitude of a_{ph} but also in its spectral nature (Figure 5A-B). A diel pattern was also evident in the spectral nature of b_{nw} but not in that of a_{dm} (Figure 5C-D). These variations are most probably indicative of phytoplankton cell growth and division as discussed elsewhere (e.g., Durand and Olson 1996).

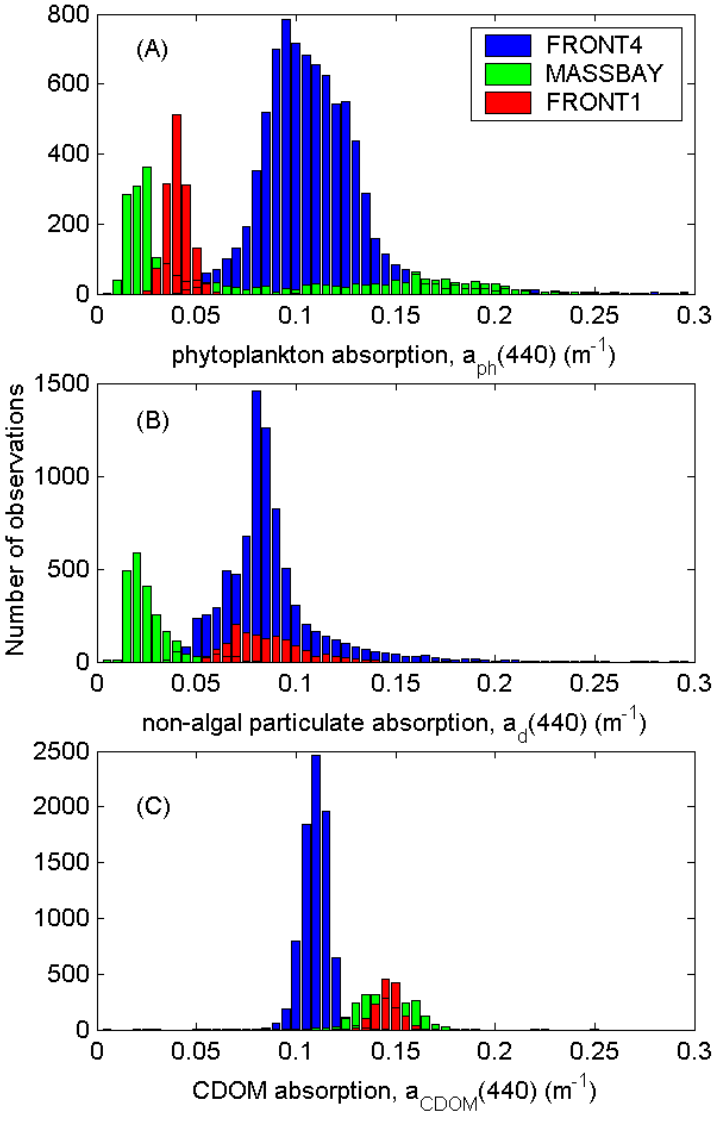

Figure 3: Distribution of optically important constituents for the three deployments as represented by their absorptions at 440 nm; A) phytoplankton, B) non-algal particulates, and C) CDOM. CDOM varied least for all three deployments but this may be the result of the calculation method which assigns the majority of variation in non-algal absorption to non-algal particulates.

CONCLUSIONS

Preliminary results indicate our new scattering correction and absorption decomposition procedure is able to correct ac-9 absorption measurements for the contribution of scattering and to provide useful information about the optically important constituents, especially phytoplankton. For both deployments at the FRONT site the scattering due to material other than water was correlated significantly with the non-algal and phytoplankton absorptions from the decomposition. We were able to estimate spectral non-algal particulate and CDOM absorption using the non-algal scattering as a proxy for non-algal particulate concentration. Optical constituent distributions showed variations on seasonal, tidal, and diel time scales. Diel variations in phytoplankton absorption properties were most probably indicative of cell division and growth and similar to previous studies.

REFERENCES

DuRand, M. D., and R. J. Olson. 1996. Contributions of phytoplankton light scattering and cell concentration changes to diel variations in beam attenuation in the equatorial Pacific from flow cytometric measurements of pico-, ultra- and nanoplankton. Deep Sea Res. **43:** 891-906.

Mitchell, B. G. 1990. Algorithms for determining the absorption coefficient of aquatic particulates using the quantitative filter technique (QFT). SPIE **1302:** 137-148.

Mobley, C. D. 1994. Light and water: radiative transfer in natural waters. Academic Press, Inc.

O'Donnell, J. 1993. Surface fronts in estuaries: a review. Estuaries **16:** 12-39.

Pegau, W. S., D. Gray, and J. R. V. Zaneveld. 1997. Absorption and attenuation of visible and near-infrared light in water: dependance on temperature and salinity. Applied Optics **36:** 6035-6046.

Roesler, C. S., M. J. Perry, and K. L. Carder. 1989. Modeling in situ phytoplankton absorption from total absorption spectra in productive inland marine waters. Limnol. Oceanogr. **34:** 1510-1523.

Simpson, J. H., and D. Bowers. 1981. Models of Stratification and Frontal Movement in Shelf Seas. Deep-Sea Res. Pt. a **28:** 727-738.

Thwaites, F. T., S. M. Gallager, C. S. Davis, A. M. Bradley, A. Girard, and W. Paul. 1998. A winch and cable for the autonomous vertically profiling plankton observatory., Oceans 98. IEEE, Piscataway, NJ (USA) Ocean Engineering Soc.

Twardowski, M. S., J. M. Sullivan, P. L. Donaghay, and J. R. Zaneveld. 1999. Microscale quantification of the absorption by dissolved and particulate material in coastal waters with an ac-9. Journal of Atmospheric and Oceanic Technology **16:** 691-707.

Ullman, D. S., and P. C. Cornillon. 1999. Satellite-derived sea surface temperature fronts on the continental shelf off the northeast U.S. coast. J. Geophys. Res. **104:** 23459-23478.

Zaneveld, J. R. V., J. C. Kitchen, and C. Moore. 1994. The scattering error correction of reflecting-tube absorption meters. SPIE Ocean Optics XII **2258:** 44-55.

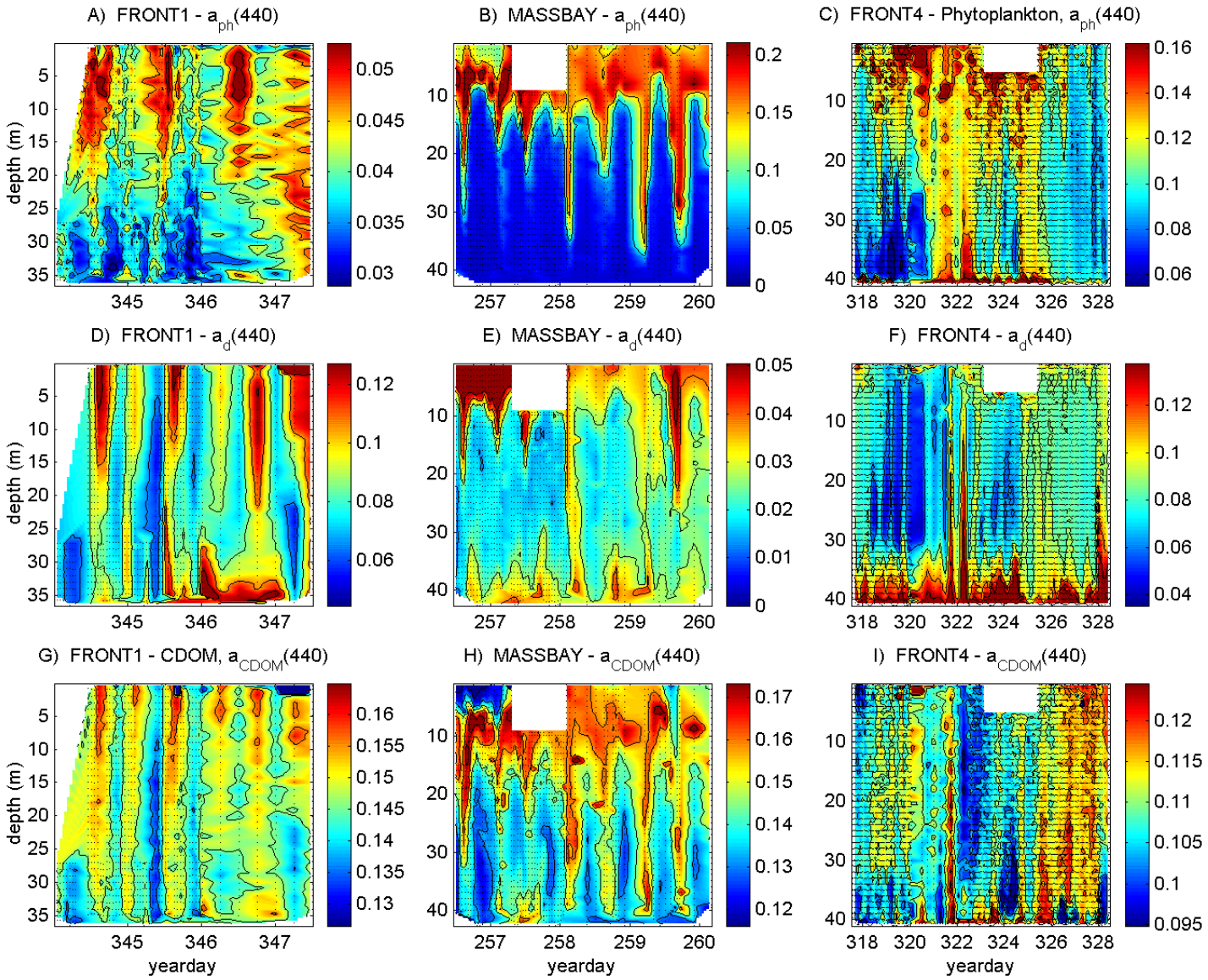

Figure 4: Interpolation of constituent absorptions with depth and time for the three deployments. Small black markers indicate the positions of measurements.

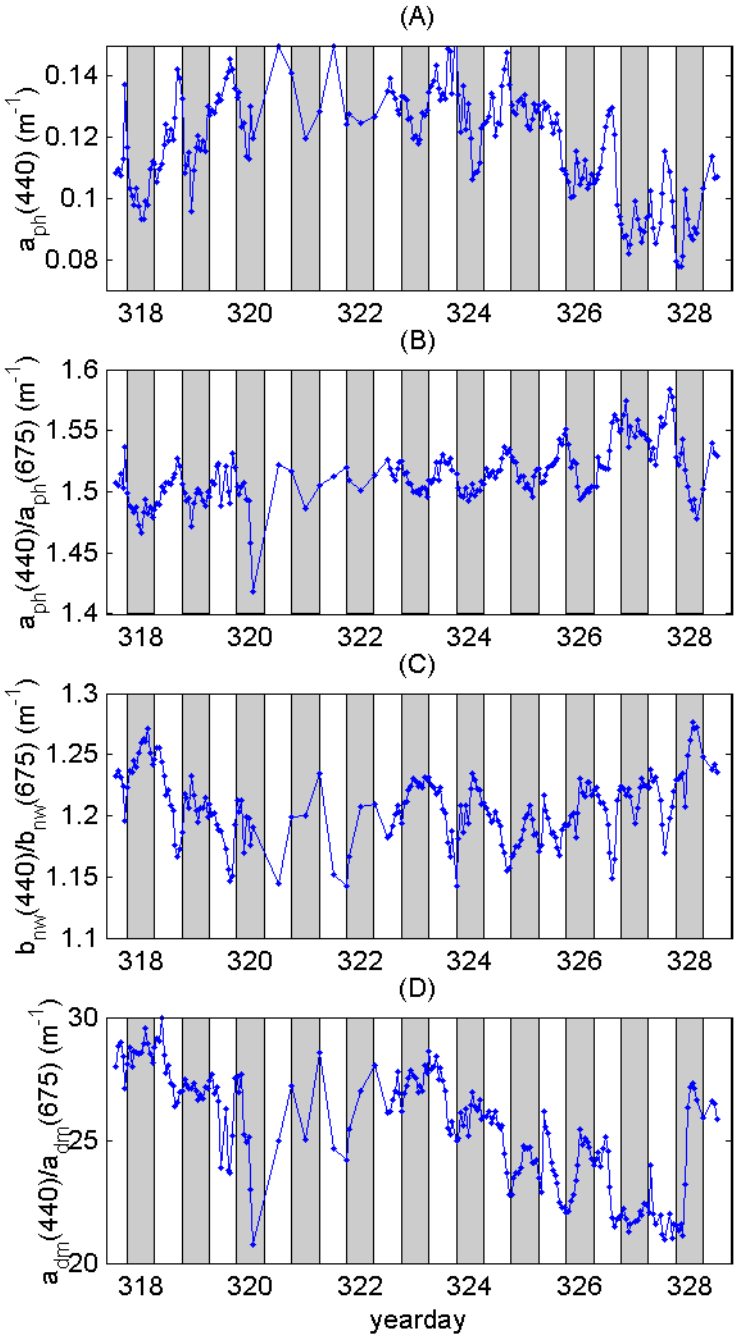

Figure 5: Time series of selected mean optical properties in the top 20 m of the FRONT4 deployment. A) Phytoplankton absorption at 440 nm, B) the ratio of phytoplankton absorption at 440 to 675 nm, C) the ratio of the non-water scattering at 440 and 675 nm, and D) the ratio of non-algal absorption at 440 to 675 nm. The gray bands are representative of the day-night cycle and not based on irradiance measurements. The first three panels clearly show a diel pattern probably associated with phytoplankton cell growth and division which is not apparent in the fourth panel.